Photoelectrochemistry of Some Organochromium Carbonyl Compounds

Richard G. Compton,*[a] Roula Barghout,[a] John C. Eklund,[a] Adrian C. Fisher,[a] Stephen G. Davies,[b] Michael R. Mètzler,[b] Alan M. Bond,[c] Ray Colton[c] and Jacky N. Walter[c]
[a] *Physical Chemistry Laboratory, Oxford University, South Parks Road, Oxford OX1 3QZ, UK*
[b] *Dyson Perrins Laboratory, Oxford University, South Parks Road, Oxford OX1 3QY, UK*
[c] *Department of Chemistry, La Trobe University, Bundoora, Victoria 3083, Australia*

The *dual* photochemical and electrochemical activation of three different organochromium carbonyl species have been studied. For each of $[Cr(CO)_6]$, *trans*-$[Cr(CO)_2(dppe)_2]^+$ [dppe = 1,2-bis(diphenylphosphino)ethane] and $[Cr(CO)_3(\eta^6\text{-}C_6Et_6)]$ the photo-oxidation has been studied and it is demonstrated that the course of the reaction in the presence of light, and its kinetics, may be studied using channel-electrode voltammetry. In the case of $[Cr(CO)_6]$ and $[Cr(CO)_3(\eta^6\text{-}C_6Et_6)]$ electron transfer to the electrode follows photochemical reaction and it is shown that the occurrence of photosubstitution in the former, and photofragmentation in the latter modifies the pathway of the electrode reaction. For *trans*-$[Cr(CO)_2(dppe)_2]^+$ photochemical reaction is only seen after electro-oxidation and this is demonstrated to lead to a disproportionation reaction.

Photochemical and electrochemical activation of organometallic molecules in fluid solution have been widely used *separately* to bring about chemical reaction, on the one hand through electronically excited states and on the other through change of oxidation state. It is therefore to be expected that *sequential* use of electrochemical and photochemical activation in the *same* experiment may lead to: (*i*) novel mechanistic pathways, (*ii*) the discovery of new compounds associated with unusual reactive intermediates, and (*iii*) new synthetic routes. Moreover the use of appropriate voltammetric techniques should simultaneously permit the identification of reaction intermediates and products and the quantification of reaction rates and/or quantum yields.

All of the above observations and measurements have been realised in the context of organic molecules.[1-6] However the ready accessibility of both differing oxidation states and the plethora of low-lying excited electronic states lead one to expect that organometallic systems will be even richer in photoelectrochemical phenomena. In this paper we generalise a preliminary report[7] and exemplify the above ideas using several organochromium carbonyl species as model compounds and present examples where the photochemical step preceeds or succeeds the electrochemical process with modification of the reaction seen in the absence of light. Channel-electrode voltammetry, as illustrated in Fig. 1, is used for our photoelectrochemical studies since it (*i*) can be readily adapted for photochemistry, (*ii*) can be coupled with independent spectroscopic techniques, and most importantly, (*iii*) permits quantitative mechanistic study *via* photocurrent measurements made as a function of mass transport (solution flow rate).[5-8] Three separate photo-oxidations will be studied; those of (*a*) $[Cr(CO)_6]$, (*b*) *trans*-$[Cr(CO)_2(dppe)_2]^+$ [dppe = 1,2-bis(diphenylphosphino)ethane] and (*c*) $[Cr(CO)_3(\eta^6\text{-}C_6Et_6)]$.

Experimental

All regular photoelectrochemical experiments were conducted using a platinum channel electrode made of optical quality synthetic silica to standard construction and dimensions[2-5] capable of delivering flow rates in the range 10^{-4}–10^{-1} cm^3 s^{-1}. Foils of size 4 mm × 4 mm, supplied by Goodfellow Advanced Materials (to a purity of 99.95% and thickness 0.025 mm) were used as working electrodes. Precise dimensions were determined using a travelling microscope. A silver wire pseudo-reference electrode was positioned in the flow system upstream of the channel electrode, and a platinum-gauze counter electrode was located downstream. Electrochemical measurements were made using an Oxford Electrodes potentiostat modified to boost the counter electrode voltage (up to 200 V). The silver wire reference electrode was found to be steady throughout the period of our experiments [as assessed *via* consistent values for the oxidation potential of the simple reversible one-electron couple tmpd–tmpd$^+$, (tmpd = *N*,*N*,*N*′,*N*′-tetramethyl-1,4-phenylenediamine)]. Hence potentials are reported relative to the saturated calomel electrode (SCE), +0.20 V being subtracted from the measured values to obtain the potentials quoted. Other methodological details were as described previously.[2-5] Irradiation was provided by a Wotan XBO 900 W/2 xenon arc lamp *via* a Jarrell–Ash 82–410 grating monochromator (incident power 40 mW cm^{-2}). UV/VIS measurements were made with a Perkin Elmer Lambda-5 spectrometer. Rotating-disc measurements were conducted using Oxford Electrodes equipment.

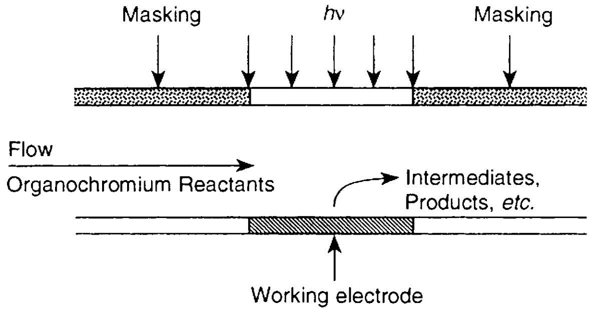

Fig. 1 A schematic diagram of a channel electrode as used for photoelectrochemical studies

Experiments were performed using solutions of the electroactive species of interest (*ca.* 10^{-4}–10^{-3} mol dm^{-3}) in dried[2] acetonitrile (Fisons, dried, distilled) solution containing 0.1 mol dm^{-3} (recrystallised) tetrabutylammonium perchlorate (Fluka, purum) as supporting electrolyte. Solutions were purged of oxygen by outgassing with prepurified argon prior to electrolysis. Hexacarbonylchromium(0) was obtained from Aldrich (> 98%).

Syntheses.—$[Cr(CO)_2(dppe)_2]$. The method of refluxing $[Cr(CO)_6]$ with 2 mole equivalents of dppe in decane[9] was used to synthesise *cis*- and *trans*-$[Cr(CO)_2(dppe)_2]$. A typical reaction time of 65 h gave a crude product which was collected by filtration, washed first with hexane and then with a small amount of dichloromethane to give red crystals of *trans*-$[Cr(CO)_2(dppe)_2]$.

The addition of methanol to a solution of the *trans* isomer in dichloromethane caused the yellow *cis*-$[Cr(CO)_2(dppe)_2]$ to separate from the solution, as previously reported.[10] The yellow product was then collected by filtration.

trans-$[Cr(CO)_2(dppe)_2]PF_6$. The previously reported method for the synthesis of complexes containing *trans*-$[Cr(CO)_2(dppe)_2]^+$ [11] was used to prepare the hexafluorophosphate analogue. A solution of KPF_6 in methanol was added slowly to a solution of either *cis*- or *trans*-$[Cr(CO)_2(dppe)_2]$ in dichloromethane (equimolar quantities). The solvent was evaporated under reduced pressure until crystallisation of the orange compound commenced. The solution was then cooled and the product collected by filtration.

$[Cr(CO)_3(\eta^6\text{-}C_6Et_6)]$. Refluxing of hexaethylbenzene with $[Cr(CO)_6]$ for 84 h followed by filtration through a short column of silica gel and recrystallisation from dichloromethane–pentane afforded the tricarbonyl chromium complex (25% yield) as yellow microneedles, m.p. 188–190 °C (decomp.).[12,13]

Results and Discussion

We consider first the photo-oxidation of $[Cr(CO)]_6$, in acetonitrile solution containing 0.1 mol dm^{-3} NBu_4ClO_4 as supporting electrolyte. Preliminary experiments were conducted in the absence of light using a platinum channel electrode to characterise the 'dark' electrochemistry. Hydrodynamic voltammetry revealed two one-electron oxidation waves with half-wave potentials, $E_{\frac{1}{2}}$, of + 1.46 and + 2.06 V (*vs.* SCE): the first wave is shown in Fig. 2. These values are in excellent agreement with the literature.[14,15] Cyclic voltammetric measurements under conditions of no-flow, at scan rates up to 200 mV s^{-1} showed that the first wave was chemically and electrochemically reversible, the second chemically irreversible. Analysis of the transport limited currents in voltammograms such as Fig. 2, as a function of mass transport (solution flow rate), permitted the deduction of the diffusion coefficient of $[Cr(CO)_6]$ as 1.6×10^{-5} cm^2 s^{-1}. This result was checked by independent rotating-disc measurements. For this, and other, quantitative work low concentrations (< 0.5 mmol dm^{-3}) were found to be essential otherwise electrode passivation precluded the recording of reproducible limiting current data.

Fig. 3 shows a hydrodynamic voltammogram analogous to Fig. 2, except that it was recorded under monochromated illumination from a xenon lamp (40 mW cm^{-2}; 320 nm). Three new oxidation waves, labelled A, B and C, are apparent at potentials less anodic than are required for the oxidation of $[Cr(CO)_6]$ in the dark. The half-wave potentials of these waves are +0.90 (A), +0.40 (B) and −0.10 V (C) (all *vs.* SCE) respectively. An action spectrum—a plot of photocurrent against excitation wavelength at fixed solution flow rate—was next measured for the prewave A, *i.e.* that closest to the dark oxidation wave. This is shown in Fig. 4. The maximum photocurrent flows when the wavelength of the light is close to 320 nm. This corresponds to a shoulder in the absorption spectrum of $[Cr(CO)_6]$ and the UV/VIS band (ε = 3870 dm^3 mol^{-1} cm^{-1}) has been attributed to a metal centred d–d transition.[16]

On the basis of the photovoltammetry, the action spectra and the UV/VIS data together with the known propensity for $[Cr(CO)_6]$ to photosubstitute MeCN for CO[15,17–19] the prewaves were attributed to: (A) $[Cr(CO)_5(MeCN)]$, (B) *cis*-$[Cr(CO)_4(MeCN)_2]$ and (C) *fac*-$[Cr(CO)_3(MeCN)_3]$. The oxidation potentials of these postulated peaks are in good agreement with those measured from the independently synthesised species.[20] If all the substituted species are formed in a stepwise manner then the electrode reaction mechanism relating to the photochemical process can be summarised by the mechanism given in equations (1)–(6). Adopting the Testa and

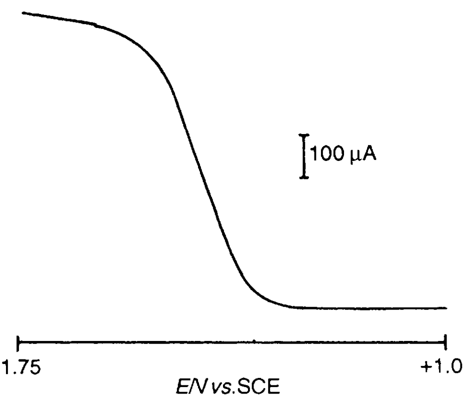

Fig. 2 A hydrodynamic voltammogram obtained in the dark at a platinum electrode from a solution of $[Cr(CO)_6]$ (1.75 mmol dm^{-3}) in 0.1 mol dm^{-3} NBu_4ClO_4–acetonitrile

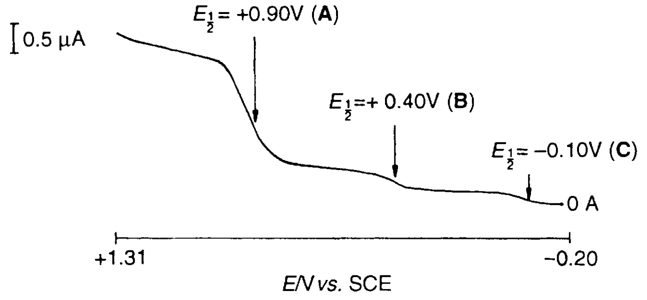

Fig. 3 A hydrodynamic voltammogram obtained at a platinum channel electrode from a solution of $[Cr(CO)_6]$ (0.17 mmol dm^{-3}) in 0.1 mol dm^{-3} NBu_4ClO_4–acetonitrile. The electrode was irradiated at 320 nm. A solution flow rate of 0.000 65 cm^3 s^{-1} was used

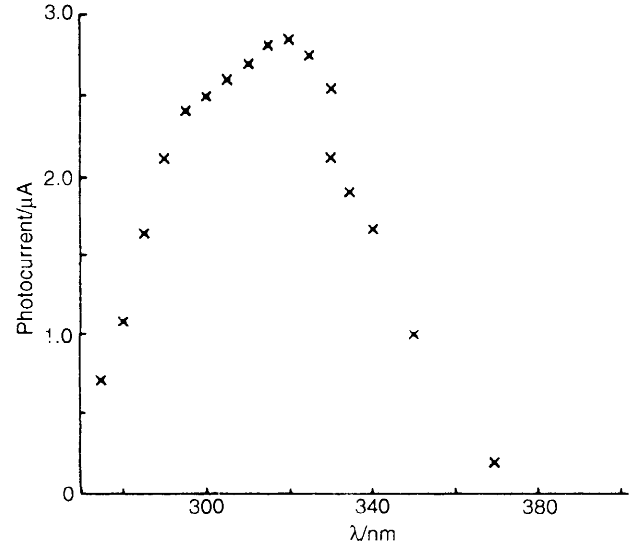

Fig. 4 An action spectrum for prewave A, formed by irradiation of $[Cr(CO)_6]$, measured at a flow rate of 0.01 cm^3 s^{-1}

$$[Cr(CO)_6] \xrightarrow[MeCN]{k_1(h\nu)} [Cr(CO)_5(MeCN)] + CO \quad (1)$$

$$[Cr(CO)_5(MeCN)] - e^- \rightleftharpoons [Cr(CO)_5(MeCN)]^+ \quad (2)$$

$$[Cr(CO)_5(MeCN)] \xrightarrow[MeCN]{k_2(h\nu)} [Cr(CO)_4(MeCN)_2] + CO \quad (3)$$

$$[Cr(CO)_4(MeCN)_2] - e^- \rightleftharpoons [Cr(CO)_4(MeCN)_2]^+ \quad (4)$$

$$\xrightarrow[MeCN]{k_3(h\nu)} [Cr(CO)_3(MeCN)_3] + CO \quad (5)$$

$$[Cr(CO)_3(MeCN)_3] - e^- \rightleftharpoons [Cr(CO)_3(MeCN)_3]^+ \quad (6)$$

Reinmuth notation[21] the three prewaves may be described as photochemical (CE) (prewave A), CECE (B) and CECECE (C) respectively.

The veracity of these mechanisms was then examined by measurement of the photocurrents associated with each prewave, at potentials corresponding to the transport-limited current for each wave, as a function of electrolyte flow rate (mass transport). It has been established that such data, taken over a wide flow rate range, provide a sensitive protocol for resolving between different possible candidate electrode reaction mechanisms.[5–8,22] The experimental data were then compared in each case with theoretical predictions based on the mechanistic models given above using the three pseudo-first-order rate constants for the photosubstitution steps as adjustable parameters. The necessary theory for computing the theoretical behaviour for these, or any other chemical models, is well established and the interested reader is directed towards the literature for the necessary details.[8,23,24] No new computational or conceptual problems emerge in their application to the present work. However it was necessary to specify values for the diffusion coefficients of all the electrochemically active species included in the proposed mechanism. As those of the acetonitrile substituted species are unknown these species were approximated by the value measured for $[Cr(CO)_6]$. This is unlikely to be in error by more than 15% and the mechanistic conclusions presented below were insensitive to variations within this limit.

All three prewaves were found to give excellent agreement with the proposed mechanism as can be seen from Fig. 5. For each wave, a wavelength of 320 nm was used corresponding to maximum total photocurrent, and good agreement across the entire flow rate range used was found for the following rate constants which relate to incident light intensities of 40 mW cm^{-2}: $k_1 = 0.146\ (\pm 0.013)\ s^{-1}$, $k_2 = 0.180\ (\pm 0.020)\ s^{-1}$ and $k_3 = 0.195\ (\pm 0.005)\ s^{-1}$. These experiments were repeated for a range of concentrations of $[Cr(CO)_6]$ between 0.1 and 0.5 mmol dm^{-3}. In each case good agreement between theory and experiment was found for this unique set of values; the quality of fit shown in Fig. 5 is representative of that obtained throughout this concentration range. Further, on conducting experiments using a range of light intensities each rate constant, k_1, k_2 and k_3, was found to be linearly dependent on the intensity, as is apparent from Fig. 6. It may be concluded that the description of the photo-oxidation of $[Cr(CO)_6]$ in terms of a CECECE process is a good one and that channel-electrode measurements are capable of quantifying the kinetics of the process. Finally we note an approximate estimate for the quantum yield, Φ_1, of photosubstitution may be found from equation (7) where k_1 is

$$k_1 = 2.303\, \Phi_1 n_0 \varepsilon \quad (7)$$

the first-order rate constant deduced from the modelling, n_0 (mol cm^{-2} s^{-1}) is the photon flux incident on the cell and ε (cm^2 mol^{-1}) is the absorption coefficient for the transition studied. With a value of $n_0 = 1.10 \times 10^{-7}$ mol cm^{-2} s^{-1} for our system[6] this gives a value of $\Phi_1 = 0.15$ (at 320 nm).

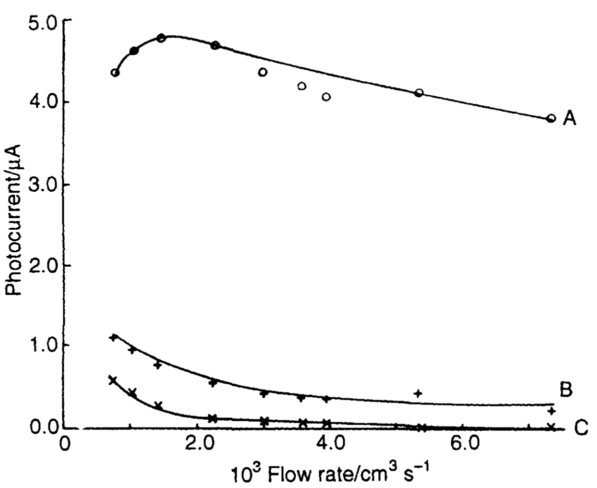

Fig. 5 Photocurrent–flow rate data for the three prewaves associated with illumination of $[Cr(CO)_6]$ with light of wavelength 320 nm. The different waves are A (○) (uppermost), (B) (+) and C (×) (lowest). The three curves relate to $[Cr(CO)_6] = 0.48$ mmol dm^{-3} and light intensity 40 mW cm^{-2}. The solid lines in each case represent the theoretical behaviour calculated from the model outlined in the text

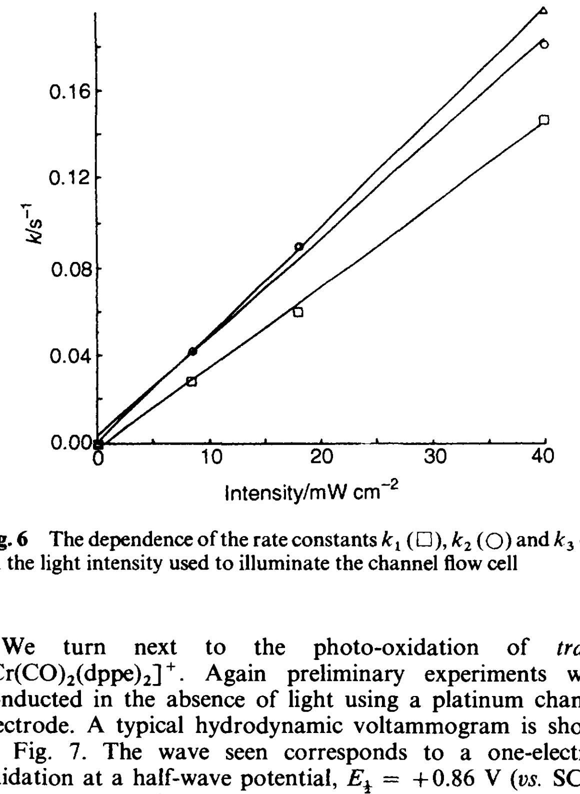

Fig. 6 The dependence of the rate constants k_1 (□), k_2 (○) and k_3 (△) on the light intensity used to illuminate the channel flow cell

We turn next to the photo-oxidation of *trans*-$[Cr(CO)_2(dppe)_2]^+$. Again preliminary experiments were conducted in the absence of light using a platinum channel electrode. A typical hydrodynamic voltammogram is shown in Fig. 7. The wave seen corresponds to a one-electron oxidation at a half-wave potential, $E_{\frac{1}{2}} = +0.86$ V (*vs.* SCE). Measurements of the mass transport-limited current as a function of electrolyte flow rate gave a value of 1.15×10^{-5} cm^2 s^{-1} for the diffusion coefficient of this species. Also shown in Fig. 7 is the voltammogram seen when the electrode is irradiated with light of wavelength 380 nm. Appreciable photocurrents are seen at potentials corresponding to the oxidation of *trans*-$[Cr(CO)_2(dppe)_2]^+$. An action spectrum was recorded by scanning the wavelength of the light incident on the cell and this is shown in Fig. 8 which reveals a maximum at 380 nm. Comparison of this with the UV/VIS spectrum of the parent compound, *trans*-$[Cr(CO)_2(dppe)_2]^+$, (λ_{max} 412 nm, ε 1620 dm^3 mol^{-1} cm^{-1}) reveals a marked difference and, since no photocurrents flow before the oxidation wave, it may be concluded that the light at 380 nm

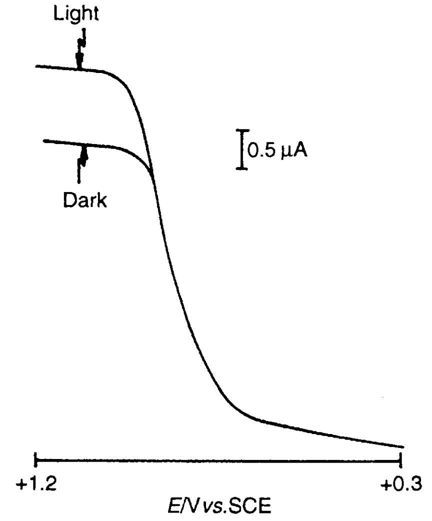

Fig. 7 A hydrodynamic voltammogram obtained from the oxidation of *trans*-$[Cr(CO)_2(dppe)_2]^+$ (of concentration 0.12 mmol dm^{-3}) in 0.1 mol dm^{-3} NBu_4ClO_4–acetonitrile. The lower line is that measured in the dark while the upper line is that seen when the electrode is irradiated with light of wavelength 380 nm. A solution flow rate of 0.0033 cm^3 s^{-1} was used

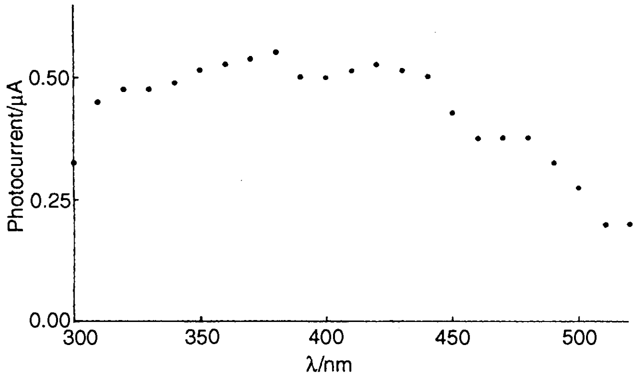

Fig. 8 An action spectrum corresponding to photocurrents formed by irradiation of *trans*-$[Cr(CO)_2(dppe)_2]^+$ (0.12 mmol dm^{-3}) recorded at a potential of +1.20 V (*vs.* SCE) corresponding to the electro-oxidation to the dication

is absorbed by the cation, *trans*-$[Cr(CO)_2(dppe)_2]^{2+}$, resulting from electro-oxidation.

The nature of the process induced by photolysis at 380 nm was investigated by means of photocurrent–mass transport measurements. Voltammograms were recorded for different concentrations of substrate between 0.09 and 0.17 mmol dm^{-3} (higher concentrations were precluded because of electrode passivation and the need to ensure negligible reduction of the incident light intensity through absorption before reaching the electrode; lower concentrations showed photocurrents too small for quantitative investigation) over the full range of flow rates available and photocurrents quantified. This data was then modelled, as before, using the diffusion coefficient reported above for *trans*-$[Cr(CO)_2(dppe)_2]^+$ and assuming that the same value approximated for the dication. The mechanism given by equations (8)–(10) gave an excellent fit with all data measured.

$$trans\text{-}[Cr(CO)_2(dppe)_2]^+ \rightleftharpoons [Cr(CO)_2(dppe)_2]^{2+} + e^- \quad (8)$$

$$2[Cr(CO)_2(dppe)_2]^{2+} \xrightarrow{k_4} [Cr(CO)_2(dppe)_2]^+ + [Cr(CO)_2(dppe)_2]^{3+} \quad (9)$$

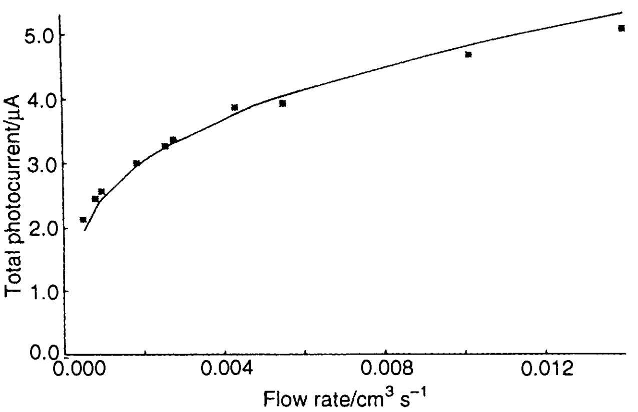

Fig. 9 Photocurrent–flow rate data for the oxidation wave of *trans*-$[Cr(CO)_2(dppe)_2]^+$ measured in 0.1 mol dm^{-3} NBu_4ClO_4–acetonitrile with the channel electrode illuminated with light of wavelength 380 nm (light intensity 40 mW cm^{-2}). The solid line shows the theoretically predicted behaviour calculated using the disproportionation mechanism and rate constants suggested in the text

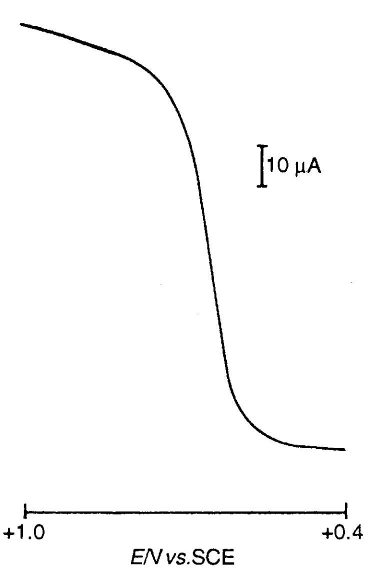

Fig. 10 Hydrodynamic voltammogram obtained from the oxidation of 0.16 mmol dm^{-3} $[Cr(CO)_3(\eta^6\text{-}C_6Et_6)]$ in 0.1 mol dm^{-3} NBu_4ClO_4–acetonitrile at a platinum electrode

$$[Cr(CO)_2(dppe)_2]^{3+} \xrightarrow{k_5} \text{products} \quad (10)$$

Fig. 9 shows a typical fit between theory and experiment obtained for a value of $k_4 = 2 \times 10^7$ mol^{-1} cm^3 s^{-1} and k_5 assumed effectively instantaneous. These rate constants were found to fit all our photocurrent experiments and k_4 was found to depend linearly on the light intensity. It may be concluded that the photo-oxidation of *trans*-$[Cr(CO)_2(dppe)_2]^+$ proceeds *via* the disproportionation mechanism suggested.

Finally we examine the photo-oxidation of $[Cr(CO)_3(\eta^6\text{-}C_6Et_6)]$. Fig. 10 reveals that in the dark a one-electron oxidation wave is seen at $E_{\frac{1}{2}} = +0.67$ V (*vs.* SCE). A value of 1.68×10^{-5} cm^2 s^{-1} for the diffusion coefficient was deduced *via* measurements of the mass transport dependence of the limiting current. Cyclic voltammetry carried out under no-flow conditions at scan rates up to 100 mV s^{-1} showed that the oxidation was chemically reversible. It is thought that species of the type $[Cr(CO)_3(\eta^6\text{-arene})]$ usually dissociate on oxidation in the dark forming the arene and a chromium containing fragment

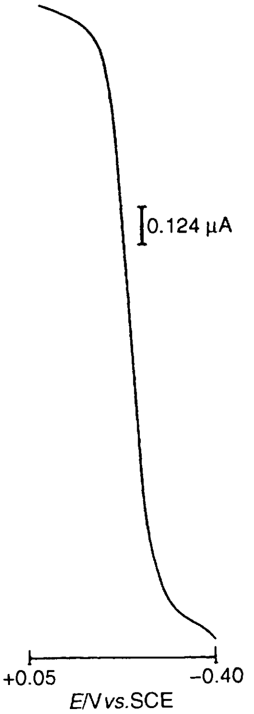

Fig. 11 Hydrodynamic voltammogram obtained from the oxidation of 0.15 mmol dm^{-3} [Cr(CO)$_3$(η^6-C$_6$Et$_6$)] in 0.1 mol dm^{-3} NBu$_4$ClO$_4$–acetonitrile at a platinum channel electrode illuminated by light of wavelength 335 nm. A solution flow rate of 0.0018 cm^3 s^{-1} was used

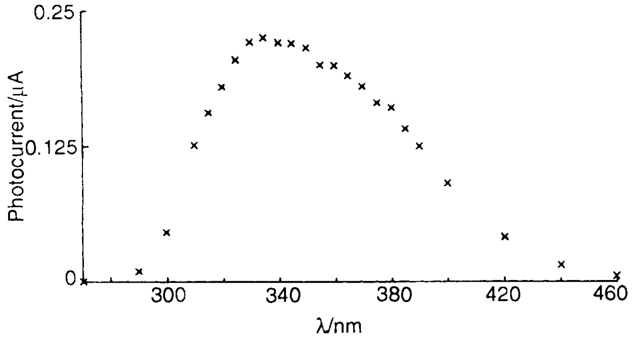

Fig. 12 An action spectrum corresponding to the transport-limited current measured on the prewave formed by irradiation of [Cr(CO)$_3$(η^6-C$_6$Et$_6$)] as a function of the wavelength of the incident light. A solution flow rate of 8.6 × 10^{-4} cm^3 s^{-1} was used

thought to be [Cr(CO)$_3$(MeCN)$_3$]$^{25-32}$ but in this case, where the arene is C$_6$Et$_6$, the cation is stable on the voltammetric time-scale due to the steric hindrance afforded to incoming nucleophiles.[31]

Fig. 11 shows a hydrodynamic voltammogram equivalent to that in Fig. 10 except that the electrode was irradiated at 335 nm. A prewave with a halfwave potential of −0.18 V (*vs.* SCE) can be seen suggesting formation of *fac*-[Cr(CO)$_3$(MeCN)$_3$] probably *via* photofragmentation into C$_6$Et$_6$ and Cr(CO)$_3$. An action spectrum recorded at a potential corresponding to the transport-limited current of this prewave is shown in Fig. 12 and displays a maximum at 335 nm which corresponds to the highest energy peak in the UV/VIS absorption spectrum of [Cr(CO)$_3$(η^6-C$_6$Et$_6$)]. The latter has been assigned to a charge-transfer (metal-to-arene) transition.[16,33] From this observation, and the noted stability on the voltammetric time-scale of the cation formed by one-electron oxidation, it is clear that the prewave results from the absorption of light by the parent [Cr(CO)$_3$(η^6-C$_6$Et$_6$)].

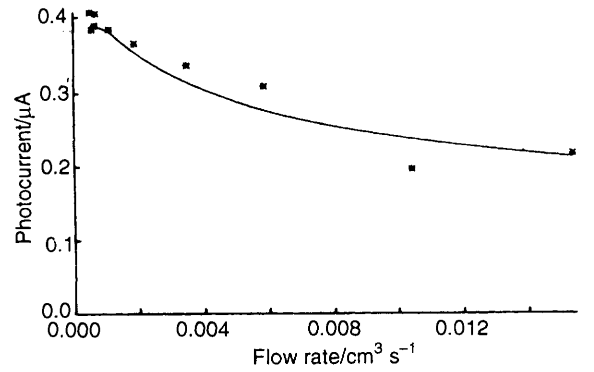

Fig. 13 Photocurrent–flow rate data for the first oxidation wave of [Cr(CO)$_3$(η^6-C$_6$Et$_6$)] measured in 0.1 mol dm^{-3} NBu$_4$ClO$_4$–acetonitrile with the channel electrode illuminated with light of wavelength 335 nm (light intensity 40 mW cm^{-2}). The solid line shows the theoretically predicted behaviour calculated using the photofragmentation mechanism and rate constant suggested in the text

Photocurrent–mass transport measurements were made to elucidate the mechanism of photo-oxidation. Again the widest possible range of flow rates was employed together with concentrations of substrate in the range 0.03 to 0.20 mmol dm^{-3}. Typical data are shown in Fig. 13. Modelling of these data was successful only for the mechanism outlined by equations (11) and (12) in which it was assumed that [Cr(CO)$_3$(MeCN)$_3$] had

$$[\mathrm{Cr(CO)_3(\eta^6\text{-}C_6Et_6)}] + h\nu + 3\mathrm{MeCN} \xrightarrow{k_6} [\mathrm{Cr(CO)_3(MeCN)_3}] + \mathrm{C_6Et_6} \quad (11)$$

$$[\mathrm{Cr(CO)_3(MeCN)_3}] \rightleftharpoons [\mathrm{Cr(CO)_3(MeCN)_3}]^+ + e^- \quad (12)$$

a diffusion coefficient similar to that of [Cr(CO)$_6$] (see above). A value for k_6 of 0.16 ± 0.02 s^{-1}, corresponding to an approximate quantum yield, Φ_6 = 0.09, was deduced and found to fit across the entire concentration range studied. It may be concluded that the photo-oxidation of [Cr(CO)$_3$(η^6-C$_6$Et$_6$)] proceeds *via* a photo–CE mechanism.

Conclusion

The three model systems studied above hint at a wealth of photoelectrochemical phenomena to be discovered in organometallic systems. The examples presented indicate the diversity of possibilities; with *trans*-[Cr(CO)$_2$(dppe)$_2$]$^+$ light drives a homogeneous electron transfer process but only after electro-oxidation whereas for [Cr(CO)$_6$] and [Cr(CO)$_3$(η^6-C$_6$Et$_6$)] photolysis precedes the electrode reaction, inducing photofragmentation and/or photosubstitution.

References

1 H. S. Carlsson and H. Lund, *Acta Chem. Scand., Ser. B*, 1980, **34**, 409.
2 U. Swanholm and V. D. Parker, *J. Am. Chem. Soc.*, 1972, **88**, 5507.
3 J. D. Moutet and G. Reverdy, *Tetrahedron Lett.*, 1979, 2389.
4 J. Erikssen, H. Lund and A. I. Nyvad, *Acta Chem. Scand., Ser. B*, 1984, **37**, 459.
5 R. G. Compton, B. A. Coles, M. B. G. Pilkington and D. J. Bethell, *J. Chem. Soc., Faraday Trans.*, 1990, 663.
6 R. G. Compton, R. G. Wellington, A. C. Fisher, D. Bethell and P. Lederer, *J. Phys. Chem.*, 1991, **95**, 4749.
7 R. G. Compton, R. Barghout, J. C. Eklund, A. C. Fisher, S. G. Davies and M. R. Metzler, *J. Chem. Soc., Perkin Trans. 2*, 1993, 39.
8 R. G. Compton, R. G. Wellington, D. Bethell, P. Lederer and D. M. O'Hare, *J. Electroanal. Chem., Interfacial Electrochem.*, 1992, **322**, 183.
9 A. M. Bond, R. Colton and J. J. Jackowski, *Inorg. Chem.*, 1975, **14**, 274.

10 J. Chatt and H. R. Watson, *J. Chem. Soc.*, 1961, 4980.

11 P. F. Crossing and M. R. Snow, *J. Chem. Soc. A*, 1971, 610.

12 R. D. Fischer, *Chem. Ber.*, 1960, **93**, 165.

13 D. J. Iverson, G. Hunter, J. F. Blount, J. R. Damewood jun. and K. Mislow, *J. Am. Chem. Soc.*, 1981, **103**, 6073.

14 C. J. Pickett and D. Pletcher, *J. Chem. Soc., Dalton Trans.*, 1975, 879.

15 C. J. Pickett and D. Pletcher, *J. Chem. Soc., Dalton Trans.*, 1976, 749.

16 G. Geoffroy and M. Wrighton, *Organometallic Photochemistry*, Academic Press, New York, 1979, ch. 2.

17 D. P. Tate, W. R. Knipple and J. M. Augl, *Inorg. Chem.*, 1962, **1**, 433.

18 G. R. Dobson, M. F. A. El Sayed, I. W. Stolz and R. K. Sheline, *Inorg. Chem.*, 1962, **1**, 526.

19 A. Seurat, P. Lemoine and M. Gross, *Electrochim. Acta*, 1978, **23**, 1219.

20 J. W. Hershberger, R. G. Klinger and J. K. Kochi, *J. Am. Chem. Soc.*, 1982, **104**, 3034.

21 A. C. Testa and W. H. Reinmuth, *Anal. Chem.*, 1961, **33**, 1320.

22 R. G. Compton, B. A. Coles and M. B. G. Pilkington, *J. Chem. Soc., Faraday Trans.*, 1988, **84**, 4347.

23 A. C. Fisher and R. G. Compton, *J. Appl. Electrochem.*, 1992, **22**, 38.

24 R. G. Compton, M. B. G. Pilkington and G. M. Stearn, *J. Chem. Soc., Faraday Trans.*, 1988, 2155.

25 M. K. Lloyd, J. A. McCleverty, J. A. Connor and E. M. Jones, *J. Chem. Soc., Dalton Trans.*, 1973, 1768.

26 T. Ikeshoji and V. D. Parker, *Acta Chem. Scand., Ser B*, 1983, **37**, 715.

27 T. Ikeshoji and V. D. Parker, *Acta Chem. Scand., Ser. A*, 1983, **38**, 173.

28 C. Degrand and A. Radecki-Sudre, *J. Organomet. Chem.*, 1984, **268**, 63.

29 K. M. Doxsee, R. H. Grubbs and F. C. Anson, *J. Am. Chem. Soc.*, 1984, **106**, 7819.

30 A. M. Bond, C. G. Zoski, D. A. Sweigart, N. A. Stone, P. H. Reiger, E. Mocellin, T. F. Mann, D. R. Mann, D. K. Gosser and M. M. Doeff, *J. Am. Chem. Soc.*, 1988, **110**, 2109.

31 J. O. Howell, J. M. Gonalves, C. Amatore, C. Klansic, R. M. Wrightman and J. Kochi, *J. Am Chem. Soc.*, 1984, **106**, 3968.

32 M. Moran, I. Cuadrado, M. C. Pascual and C. M. Casado, *Organometallics*, 1992, **11**, 1210.

33 J. Rawlings and C. A. L. Mahaffy, *Spectrosc. Lett.*, 1986, **19**, 517.

Received 13*th August* 1993; *Paper* 3/04922A